YALE PEABODY MUSEUM

JOURNAL OF MARINE RESEARCH

The *Journal of Marine Research,* one of the oldest journals in American marine science, published important peer-reviewed original research on a broad array of topics in physical, biological, and chemical oceanography vital to the academic oceanographic community in the long and rich tradition of the Sears Foundation for Marine Research at Yale University.

An archive of all issues from 1937 to 2021 (Volume 1–79) are available through EliScholar, a digital platform for scholarly publishing provided by Yale University Library at https://elischolar.library.yale.edu/.

Requests for permission to clear rights for use of this content should be directed to the authors, their estates, or other representatives. The *Journal of Marine Research* has no contact information beyond the affiliations listed in the published articles. We ask that you provide attribution to the *Journal of Marine Research.*

Yale University provides access to these materials for educational and research purposes only. Copyright or other proprietary rights to content contained in this document may be held by individuals or entities other than, or in addition to, Yale University. You are solely responsible for determining the ownership of the copyright, and for obtaining permission for your intended use. Yale University makes no warranty that your distribution, reproduction, or other use of these materials will not infringe the rights of third parties.

Foam triangles

by S.A. Thorpe[1]

ABSTRACT

Foam patches left by waves breaking as they approach a smooth and gently sloping beach from a near-normal direction sometimes have the distinctly triangular shape that has been studied by Turner and Turner (2011). Explanations of the size of the angle at the apex of the triangles observed by Turner and Turner are suggested in terms of physical processes that determine the speed at which the point of breaking travels along a wave crest. These explanations differ from the entrainment model proposed by Turner and Turner (2011). The range of sizes of the apex angles can most likely be explained in terms of the directional spreading of waves approaching the surf zone.

1. Introduction

The patterns observed in foam left by breaking waves may reveal some of the physical processes involved in wave breaking and its residual turbulence (Thorpe et al. 1999a and Thorpe et al. 1999b). Here we consider the triangular patches of foam sometimes produced by breaking waves as they approach a smoothly and gently sloping beach from a near-normal direction (Thorpe et al. 1999a; Thorpe et al. 1999b; Turner and Turner 2011). Figure 1A is a photograph of foam triangles taken from Thorpe (2005), and Figure 1B is an interpretive sketch of the features in the photograph. The development of a foam triangle is shown in the sequence of photographs in Figure 2 taken from a vantage point on the West Cliff at Whitby, UK. In Figure 2A, a wave has just begun to break, leaving foam in its wake. Figure 2B shows the increased length of the breaking region as the wave advances towards shore. Figure 2C is taken just as the breaking region amalgamates with other breaking regions on its flanks, resulting in the subsequent continuous alongshore band of foam in Figure 2D.

Figure 3 is a sketch of a foam triangle with points marked for future reference. A wave crest beings to break at some particular position near A in Figure 3, this location being determined by a slight irregularity in amplitude as a wave approaches breaking, perhaps caused by waves crossing the main (primary) wave as discussed later. (Often the initial breaking is along a small length of the wave crest, leading to "flat topped" foam triangles.) The wave in the breaking region (BC) may be described as a continuously spilling wave

1. School of Ocean Sciences, Bangor University, Menai Bridge, Anglesey LL59 5AB, UK. Address for correspondence: 'Bodfryn', Glanrafon, Llangoed, Anglesey LL58 8PH, UK. *e-mail: oss413@sos.bangor.ac.uk*
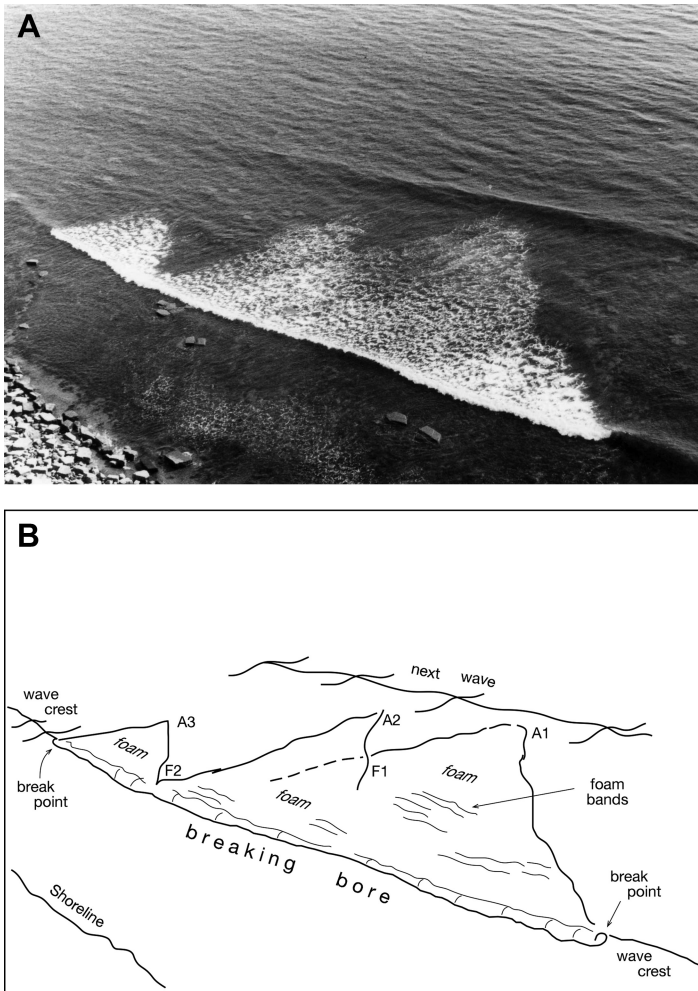
Figure 1. **A:** Triangular foam patches, photograph by N. Walters and included in his undergraduate dissertation, "The dispersion of foam produced by breaking waves in the surf zone," Southampton University, U.K., 1995. **B:** Interpretive sketch of **A**.

leaving foam in its wake as observed by Turner and Turner (2011), or as a hydraulic jump or turbulent bore. For brevity, we simply refer to it as a "bore." At the two points, B and C in Figure 3, referred to later as the break points of the breaking crest, the wave continually breaks, either by spilling (as observed by Turner and Turner) or by plunging as in Figure 2A and 2B with a forward-moving jet of water advancing from the wave crest falling and impacting with the water ahead of the crest, so forming the end of a short tube of air beneath the overhanging jet, a location favored by surfboarders and often shown in dramatic films of wave breaking.
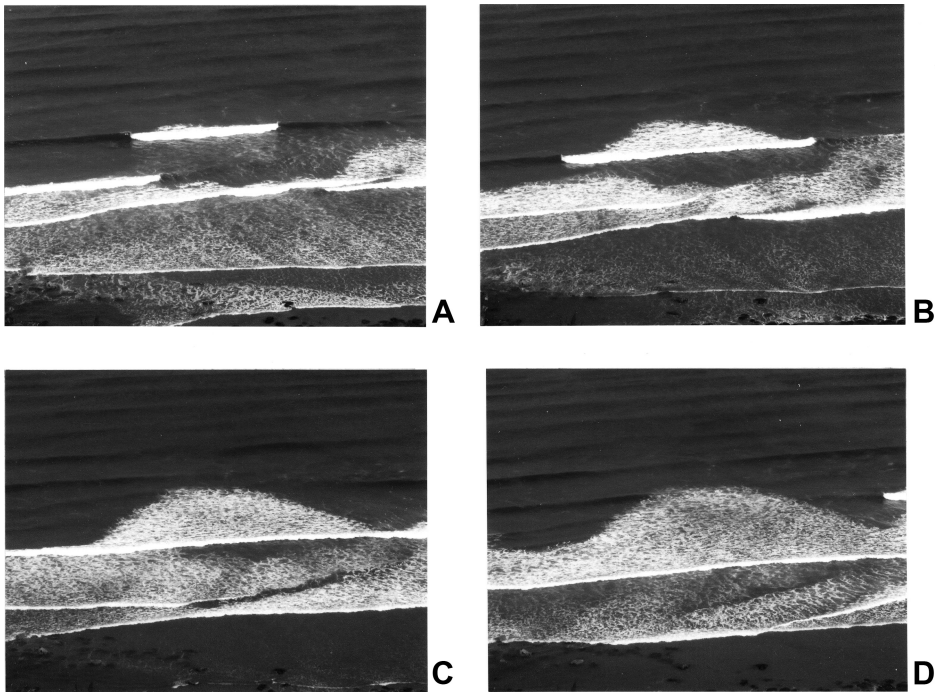
Figure 2. A sequence of photographs at about 2.8 s intervals of a breaking wave approaching a smooth sandy beach and producing a foam triangle. **A:** the wave has just begun to break, leaving foam in its wake. **B:** the extent of the breaking crest or bore and the foam has increased and at **C:** amalgamates with breaking regions in the same wave on the flanks of the original breaker. The relative location of the images taken with a hand-held camera has been fixed by rocks on the shoreline. Superposition of the photographs shows that the foam near the apex of the foam triangle persists in its position during the sequence of photographs. During this period, there is no along-shore movement or spread of the foam triangles once formed and the foam does not drift towards shore. The center of the breaking region moves linearly towards shore indicating an approximately equal but opposite rate of spread at the two break points.

Foam produced in the process of wave breaking persists and remains on the water surface behind the advancing bore, forming the observed triangular shape, ABC in Figure 3, with its apex, A, at or close to the location of the initial breaking. The base of the triangle, BC, is the turbulent bore. The lines continuing to the left and the right of B and C, respectively, mark the yet unbroken wave crest. The two sides, AB and AC, are the edges of the region of foam and turbulence generated by the breaking wave. Foam is generated along the front of the breaking bore; to a first approximation, the foam triangle is the region swept out by the break points of the breaking wave. The (possibly differential) advection resulting from the movement of water on which the foam floats, the disappearance of foam or its decay, and its turbulent spread, are found to be small when the images of Figure 2 are superimposed,
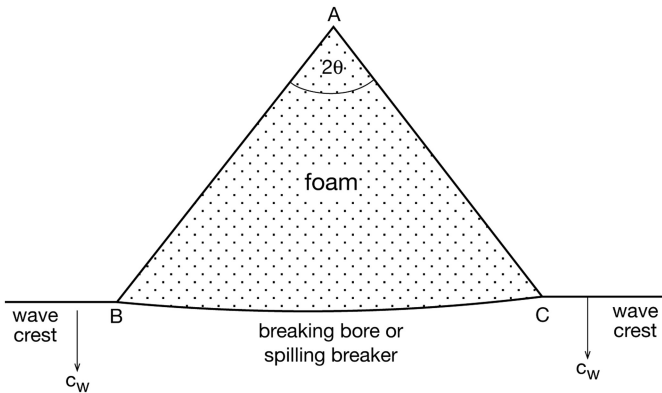
Figure 3. Notational sketch showing a triangular foam patch being generated by a breaker.

and are regarded here as secondary effects. At the time of the photographs, Figure 1A and Figure 2A and 2B, the waves following those producing the foam triangle have not entered the region ABC of the triangle, i.e., the following waves have not passed the location at which breaking first occurs, the apex of the largest (and oldest) triangle A1 in Figure 1B; a second wave has not entered the region ABC of the foam triangle.

"The angle of the apex of the foam triangle is determined by the ratio of the" (lateral) "speed of movement of the break-point along the wave crest to the speed of advance of the" (breaking) "wave towards shore" (Thorpe et al. 1999a, 328). This ratio is a parameter r, called the entrainment ratio by Turner and Turner (2011). It is equal to $\tan\theta$ where 2θ = angle BAC in Figure 3. Turner and Turner analyze 20 photographs of foam triangles in locations where wave breaking occurred at depths, D, of 4.35 m to 7.70 m. In a water depth of approximately 10 m (at low tide, but in a location 9 km away) waves had significant wave heights, H_s, in the range 0.58 m to 2.23 m, and peak wave periods, T_p, from 5.9 s to 14.3 s at the time of the photographs. The best-fit for the angle θ estimated from the photographs is 33°, giving an average $r = 0.65$. The values of r, however, span a range from 0.50 to 1.07, corresponding to $26° < \theta < 47°$. No systematic variation of r with D, H_s, T_p or with H_s divided by the peak wavelength, are found. Small asymmetries in the foam triangles are explained as a consequence of along-shore currents in the surf zone.

Turner and Turner (2011) explain the formation of the foam triangles in terms of entrainment resulting from instability caused by the difference in surface flow between the part of a spilling wave crest that is sharp (and where aerated water or foam is carried ahead of the crest) and where it is rounded (allowing aerated water to flow over it). No quantitative prediction of the size of r is obtained. However, if turbulence is characterised by a turbulent velocity, u', roughly proportional to (but probably smaller than) the speed of the wave, c_w, then the rate of entrainment of quiescent fluid into the foam region (diluting the foam and contributing to its indistinct edge) is about $E_n c_w$, where E_n is an entrainment coefficient. Such coefficients are typically of order 0.1, suggesting that the sides of the foam triangle

will spread outwards in directions normal to AB and AC at speeds substantially less than the speed of the wave. (As already noted, however, no lateral spreading of the foam triangle is apparent in the set of photographs, although the boundaries, AB and AC of the foam triangles show some evidence of less intense foam, consistent with its dilution or its reduction by bubble bursting and amalgamation.) A speed, $E_n c_w$, normal to AC contributes to a motion in direction BC along the breaking wave crest, i.e., an along-crest speed $E_n c_w / \cos\theta$. This implies $r = E_n / \cos\theta$ or $r \sim 0.12$ if $E_n \sim 0.1$ and $\theta \sim 33°$, too small to explain the observed range, $0.5 \leq r \leq 1.07$, unless E_n is a factor of 5–9 greater. Entrainment therefore appears an unlikely explanation of the spreading rate; another is needed.

2. Directional spread

Low frequency or swell waves in deep water are known to have a directional spreading angle about the mean propagation direction. This depends on the waves' history, particularly on the steadiness or variability of the wave-forcing wind. The observed spreading angles are typically in the range $10°-30°$ (see for examples Herbers et al. 1999; Herbers et al. 2003; Petterson et al. 2003; Hisaki 2005; Henderson et al. 2006; Cheed and Hay 2008), and wave directional spectra are roughly symmetrical about the mean direction. Bimodal distributions are found after changes in wind direction (Kuik et al. 1988). The spreading angles decrease as waves approach the outer edge of the surf zone (in accord with Snell's law for bathymetric refraction), before increasing during shoreward propagation across the surf zone (Herbers et al. 1999; Herbers et al. 2003; Henderson et al. 2006).

Directional spreading may provide an explanation of the generation of foam triangles as follows: suppose, for simplicity, that the directional spread is represented by the three waves shown in Figure 4, a larger primary (crest line BC) that is propagating directly towards shore along line AD in Figure 4, and two smaller secondary waves (crest lines EC and FB) travelling at angles $\pm\phi$ to the primary. It is usually appropriate to treat the shallow-water waves as solitary waves (Peregrine 1983). Tanaka (1986) shows that the wave energy density of a solitary wave first reaches a maximum and the wave becomes unstable when $h_1 = 1.782 h_0$ and $c_w = 1.294 (g h_0)^{1/2}$ (Tanaka 1986), where h_0 is the depth of water into which the wave is propagating and h_1 is the height of the wave crest above the seabed; breaking may then ensue (Tanaka et al. 1987). We therefore assume that the primary wave is of finite amplitude and speed less than $c_w = 1.294 (g h_0)^{1/2}$, and that the smaller secondaries have speeds, c_1, that are equal to or exceed that of a small amplitude solitary wave, $(g h_0)^{1/2}$, but substantially less than c_w.

Wave breaking is initiated at the point A in Figure 4 where the crests of the three waves cross and where the height of the surface is a maximum, resulting in a height to depth ratio exceeding that necessary (order unity) for breaking to occur. Breaking of the primary continues to be initiated where its height is supplemented by the crests of the two secondary waves. At a time, t, after first breaking, as shown in Figure 4, the secondary waves crests (EC and FB) have advanced distances AE and AF ($= c_1 t$) less than that, AD ($= c_w t$), of
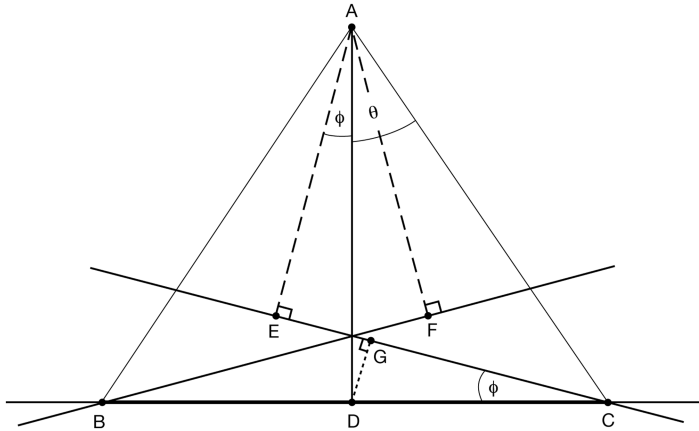
Figure 4. The interaction of a primary wave and two smaller secondaries. The secondaries propagate at angles $\pm\phi$ to a larger primary that is propagating parallel to the line AD, towards shore. Full lines represent wave crests at a time, t, after breaking of the primary is initiated at A where the wave height is increased by the presence of the crossing secondaries. After the time, t, the primary wave crest lies along BDC and the secondary crests are EB and FC at distances $AD = c_w t$ and $AE = AF = c_1 t$ from A. Angles EAD and FAD are equal to ϕ. Breaking of the primary along BC is produced by the local enhancement of its wave height by the secondaries, and results in the foam triangle, ABC, with apex angle, θ, as in Figure 3. The point G is the foot of the perpendicular from D to the secondary wave crest, EC.

the primary wave. As a result of the interactions, the primary wave crest is breaking along the line BDC, and since the breaker points, B and C, advance at speed c_{break}, $DC = c_{break}t$. Since $DG = DC\sin\phi = AD\cos\phi - AE$, where G is the foot of the perpendicular from D to the secondary wave crest, EC, it follows that

$$c_{break} \sin\phi = c_w \cos\phi - c_1, \tag{1}$$

where $c_{break} = c_w \tan\theta = rc_w$, or

$$r = \cot\phi - 1/(c_w/c_1) \sin\phi. \tag{2}$$

This can be cast as a quadratic equation in $s = \tan(\phi/2)$ and solved to obtain ϕ as a function of r and c_w/c_1. Supposing that $c_w/c_1 = 1.29$, the maximum ratio of primary to secondary wave speeds, we find that $19.5° > \phi > 11.1°$ when r is in the range 0.5 to 1.07 (or $26° < \theta < 47°$) observed by Turner and Turner (2011). Alternatively, for a relatively larger and faster secondary, if $c_w/c_1 = 1.15$ we find $12.3° > \phi > 6.62°$. These ranges of ϕ are consistent with those commonly observed; the observations of Turner and Turner of the range of r is in accord with the typical directional spreading of waves. The observed and predicted apex angles of foam triangles generally exceed the spread of wave directions. Remarkably, as can be seen from Figure 4 or by taking the ϕ derivative of (2) with $r = \tan\theta$, the apex
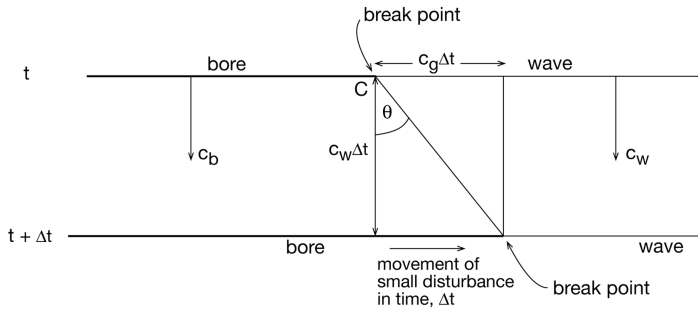
Figure 5. The spreading of a disturbance along the near-breaking wave crest at speed c_g when the bore and the wave speeds are equal. The horizontal thin and thick lines indicates the wave crest and the bore, respectively, at times t (when the break point is at C) and at a later time, $t + \Delta t$.

angle, θ, and $r (= c_{break}/c_w)$ increase as the directional spread, ϕ, decreases; the breaking points of waves with a narrow directional range spread relatively rapidly along their crest.

There are, however, several uncertainties in this argument. It assumes that the secondary wave crests are sufficiently long (or coherent) during propagation for the break points to move continuously and steadily along the primary wave crest as suggested in Figure 4. The spread in wave directions is a statistical concept, resulting in a stochastic process that may not be properly represented by a primary with two secondary waves. Wave breaking in the surf zone is strongly affected by the presence of wave groups approaching shore from deep water (e.g., Thorpe and Hall 1993), and it is only the directional spreading angles of larger waves in such groups, and not of all long waves, that should be represented in the argument. No account is given to the three-dimensional dynamical processes operating at the break points. Nevertheless, it appears likely that the argument encompasses the main features of the effect of directional spreading, and (whilst definitive observations appear to be lacking) that directional spreading accounts for the range of θ or r in observed by Turner and Turner (2011).

Other possible explanations of the ratio, r, are presented below.

3. Other explanations of the size of r

Disregarding the directional spread of waves, the parameter r may possibly be determined by other physical processes leading, locally, to the movement of the break point along the wave crest.

a. Energy transfer along the wave crest

Suppose that the movement of the break point along the unbroken wave crest (e.g., to the right at point C in Figure 3) is triggered by a small gravity wave disturbance, caused by the wave's breaking, that moves along its crest as shown in Figure 5. The rate of transport
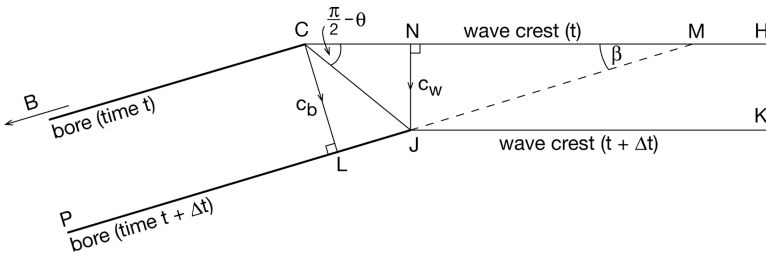
Figure 6. The lateral advance of the convex bore front along the unbroken wave crest. The position of the unbroken wave and bore are shown at times t and $t + \Delta t$. In this time the break point moves from C to J.

of the wave energy or of "information from the breaker region" is equal to the wave group velocity, c_g. In linear gravity wave theory c_g is given by

$$c_g/c = 0.5(1 + 2kD/\sin h2kD), \tag{3}$$

(Phillips 1966), where $c = [(g\tanh kD)/k]^{1/2}$ is the phase speed of a wave of wavenumber, k, in water of depth, D. The group velocity ranges from $0.5c = 0.5(g/k)^{1/2}$ for short waves in deep water (as kD tends to infinity and when $c = (g/k)^{1/2}$), to $c = (gD)^{1/2}$ for long shallow water waves (as kD tends to zero and c tends to $(gD)^{1/2}$). If the water depth on the near-breaking wave crest is h_1, then the speed of spread of the short 'trigger' waves, c_g, lies between $0.5(g/k)^{1/2}$ with $k >\sim 2h_1^{-1}$, and $(gh_1)^{1/2}$. The speed of the break point along the wave crest, $c_{break} = c_g$, and the ratio r is

$$r = c_g/c_w. \tag{4}$$

An upper limit may be placed on the speed, c_w, of near-breaking waves on a gently sloping beach. Using the maximum solitary wave speed prior to breaking, $c_w = 1.294(gh_0)^{1/2}$ (Tanaka, 1986) described in Section 2, the maximum (long wave) velocity of a small disturbance along the wave crest is $c_g = (gh_1)^{1/2} = 1.335(gh_0)^{1/2}$, so that $r = c_g/c_w$ is about 1.03, providing an approximate upper bound for r close to that, 1.07, observed by Turner and Turner (2011). (The maximum $c_g \propto h_1^{1/2}$, so $c_g \propto c_w$, $\propto h_0^{1/2}$, and the spreading angle, θ, remains constant as h_0 decreases. The sides, AB and AC, of the foam triangle are therefore straight lines; see Appendix A, a.) However, with the same values of h_1 and c_w, a value $r = 0.5$, corresponding to the lower end of the observed range, is found for small disturbances with wavelength of $7.1h_0$. The disturbance wavelengths appear to be unreasonably long.

b. Curvature of the front of the 'bore'

The base of foam triangles is sometimes observed to be curved, convex towards shore (an example is shown in Turner and Turner's (2011) photograph, figure 6). While this may, in some cases, be a consequence of variable along-shore bathymetry, can it imply that the

bore may advance more rapidly than the crest of the unbroken wave beyond the breaker region, i.e., to the left of B and right of C in Figure 3? If h_2 is the water depth behind the bore travelling into still water of depth h_0, a balance across the front of a bore of pressure force and rate of increase in momentum leads to a bore speed given by

$$c_b = [gh_2(h_2 + h_0)/2h_0]^{1/2}, \qquad (5)$$

(Lighthill 1978). This increases as the bore height, $h_2 - h_0$, increases for given h_0. For a turbulent and breaking (rather than undular) bore propagating into water of depth h_0, it is found empirically that $h_2/h_0 > 1.3$ or that c_b must exceed about $1.23(gh_0)^{1/2}$. This should apply here since no following waves are evident in the photographs of the bore. If the wave crest (the region outside the section BC in Figure 3) and the bore front (BC) advance at equal speeds then, as in Section 2, $c_b = c_w = 1.294(gh_0)^{1/2}, > 1.23(gh_0)^{1/2}$, and it may be expected that the "bore" will be turbulent, as indeed observed. The wave and bore speeds are equal when the water depth in the foam area behind the bore, h_2, is equal to $1.396h_0$. This is less than the crest height, $h_1 = 1.782h_0$; the water depth behind the bore is then much less than that at the crest of the wave.[2] The bore speed exceeds that of the solitary wave when $h_2 > 1.396h_0$. Since, by (5), the bore speed depends on its height, $h_2 - h_0$, curvature of the bore may reflect variation in the height of the bore, being greater near its centre (i.e., halfway between the points B and C, perhaps because a higher bore is formed where waves break in deeper water nearer point A).

A convex shape of the bore implies that near B and C in Fig. 3 the normal to the bore front is not normal to the unbroken wave (outside the section BC); the bore front makes some angle, β, with the unbroken wave crest, and the bore spreads its convex surface with a component of velocity along BC. The junction, C, of the wave (CM) and the bore (CB) is shown in Figure 6 at some time t as the wave advances and, in breaking, it forms the bore. After a further time Δt the wave is at JK and the bore lies along JP. The rate at which the breaker point C moves along the wave crest, c_{break}, is shown in the Appendix B to be

$$CN/\Delta t = c_{break} = (c_b - c_w \cos \beta)/\sin \beta, \qquad (6)$$

where as before c_b is the speed of the bore and c_w the speed of the unbroken wave. The parameter, $r = c_{break}/c_w$, is therefore

$$r = [(c_b/c_w) - \cos \beta]/\sin \beta, \qquad (7)$$

so that r depends on the intersection angle, β, and the ratio c_b/c_w. Writing (7) as

$$c_b/c_w = r \sin \beta + \cos \beta, \qquad (8)$$

---

2. It would appear physically and geometrically impossible for a bore to be generated by breaking at a wave crest lower than the top of the bore. Unless there is a hydrostatic pressure gradient parallel to the shoreline that would drive a spreading of the foam triangle, the water depth behind the bore (in the foam area of Figure 3) must be approximately equal to that behind the crest of the advancing wave (i.e., to the left and right of the triangle ABC in Figure 3). The water depths ahead of both bore and wave are however equal, so implying an asymmetry of the wave profile.
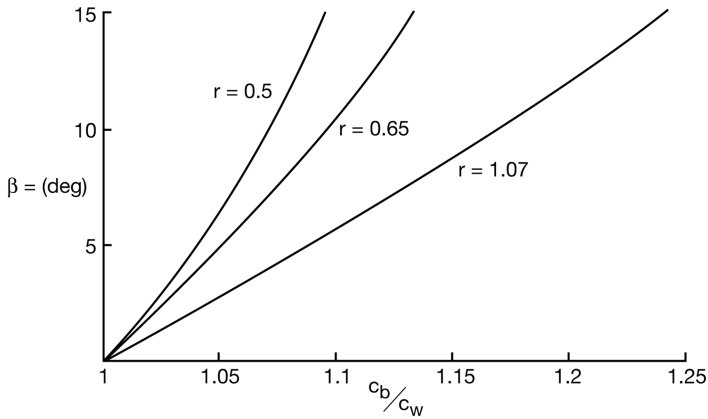
Figure 7. The variation of β with c_b/c_w for values of $r = 0.5$ and 1.07, spanning the range observed by T&T, and the mean observed value, $r = 0.65$.

the relation between c_b/c_w and β, consistent with the spreading model, can be determined for r in its observed range, 0.5–1.07, as shown in Figure 7. A value of β $\sim$ 10°, a rough estimate of the intersection angle made from Turner and Turner's figure 6, would require c_b/c_w in the range 1.07–1.17 for r to lie within its observed range. The corresponding range of depths behind the "bore" is about $h_2/h_0 = 1.52$ to 1.70. There appear to be no measurements of r, the angle β and the amplitude of the change in water depths across the bore to confirm or refute these estimates.

c. The curvature of the toe of the bore near the break points

Contrary to the above discussion, Figure 2 shows no evidence of a general curvature of the front of the bore that might indicate that $c_b > c_w$, except near the break points. Instead the figure suggests that $c_b \approx c_w$, although the forward edge of the foam in the bore, the "toe" of the bore, is positioned ahead of the wave crest; near the break points in Figure 2A and 2B, the edge of the white foaming region, the position of the toe near the break points, is curved as illustrated in Figure 8. These relative positions of the toe and wave crest are a result of foam being produced, or moving, ahead of the wave crest. Analysis in Appendix C shows that

$$\cos^2 \theta = c_w/(c_w + c_t), \tag{9}$$

where c_t is the speed of the toe of the foam relative to the wave.

Rapp and Melville's (1990) figures 8 and 9, laboratory photographs of spilling and plunging breakers (albeit of waves breaking in deep water), are used to provide estimates of c_t/c_w: the ratio is about 0.32 for the spilling wave and 0.67 for the plunging wave. Substitution into (9) gives values of $\theta = 29.5°$ and 39.3° for spilling and plunging breakers, respectively, with
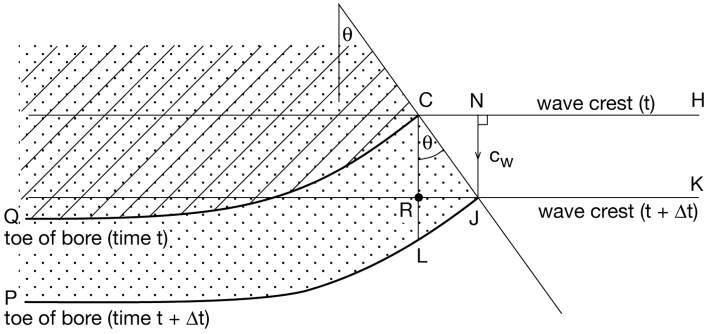
Figure 8. The advance of the wave crest and the toe of the breaking wave near a break point, C, from time t to $t + \Delta t$. The region above the toe of the bore, QC, that is both stippled and shaded, shows the foam area at time t, whilst the stippled region above PJ (including that above QC) shows the foam area at time $t + \Delta t$.

corresponding $r = 0.57$ and 0.82. These are approximate, depending on the assumptions leading to (9) and how representative are the two estimates of c_t/c_w, but they bracket the best-fit value of r found by Turner and Turner (2011).

4. Summary

As shown in Section 2, the directional spreading of waves can account for the range of the apex angles observed by Turner and Turner (2011) in foam triangles. Entrainment as proposed by Turner and Turner appears to be a less likely explanation.

Three other explanations are discussed. In the first (Section 3a) the wave crest is supposed to be parallel to the front face of the bore, and the point of breaking travels along a wave crest as a small disturbance with finite group velocity, c_g. This leads to an upper limit, 1.03, for r, near the highest value, 1.07, observed by Turner and Turner (2011). The long wavelengths of the disturbances necessary to establish the values of c_g needed to explain the observed values of r (as well as the uncertain effect of the distortion of an along-crest propagating disturbance caused by the steeply sloping sides of the near-breaking wave) place this explanation in doubt. The second explanation (Section 3b) is that the breaker point moves in a manner consistent with the curvature of the bore or front of the continually spilling wave when $c_b/c_w > 1$. This provides plausible values for r, but the curvature of the front of the bore, on which the explanation rests, appears not to be a universal feature of foam triangles. Neither of these two explanations addresses the way in which a wave breaks in three-dimensions along its crest or the details of the transmission of energy along the crest of a wave that is close to breaking. The analyses hinge on how well the near-breaking wave and the continuously breaking region, termed the "bore," can be described by theoretical results relating to a solitary wave and a hydraulic jump. The third explanation (Section 3c)

comes closer to providing a logical and quantitatively correct estimate of *r* and of its relation to the physics of wave breaking.

A study of the momentum and energy conservation in the three-dimensional transformation from wave to bore might be instructive but is not attempted here; in view of the complexity made evident by Tanaka et al.'s (1987) study in two-dimensions, it appears formidable. Further study of the directional properties of the waves approaching breaking, and photographs of the development and movement of the resulting break points might help to better establish the development of foam triangles and the physical processes involved in wave breaking.

APPENDIX A

Further discussion of the photographs

a. Wave propagation speeds

The speed of a near-breaking wave towards shore will change—probably decreasing (but depending on how its amplitude changes)—as the water depth decreases. So if the foam patches are exactly triangular, the speed of the movement of the break-point along the wave crest must be proportional to the changing speed of advance of the wave (or must have the same relation to water depth as has the wave). If the sides, AB and AC, of a foam triangle are convex inwards, this would imply an increasing ratio of spreading to wave speed, c_w (i.e., with the spreading speed possibly remaining constant as c_w decreases towards shore), and if convex outwards, away from the triangle, the spreading speed would decrease as a fraction of c_w. The edges of foam in available photographs (e.g., Figures 1 and 2) are not sufficiently distinct to establish definitely whether the sides AB and AC are curved or not, but curvature is not very evident.

b. Multiple triangles

The presence of "overlapping foam triangles" is remarked on by Turner and Turner (2011) and three such triangles, with approximately equal apex angles, are visible in Figure 1A. The apexes (points A_1, A_2 and A_3 in Figure 1B) of the triangles are outside the foam triangles of the others. The foam triangles are produced by the same shoreward-travelling wave that begins to break at different times in two or more different along-crest locations; none of the edges of the triangles is visible closer to shore than the breaking wave or bore, i.e., one triangle is not a remnant of a generation by an earlier wave being over-run by the triangle behind a new bore. The points F1 and F2 in Figure 1B at which two triangles meet marks a collision between the two bores forming the base of foam triangles originating from A1 and A2, and A2 and A3. (These collisions between waves of soliton form differ from the interactions usually considered between solitons in that the bores are not crossing one

another, but are parallel; the collisions occur end-to-end along the lengths of the waves.) The edges of the triangles originating from A1 and A2 can be detected even within the foam sheets where the two triangles overlap. These edges are marked by dashed lines extending from F1 in Figure 1B, and possibly indicate locations of more intensive breaking and foam production resulting from the collision (at F1) of bores forming the bases of two foam triangles.

APPENDIX B

An angle, β, between the wave and bore; $c_b > c_w$

Figure 6 shows the intersection of the bore or front of a continually spilling wave and the unbroken wave near break point C. The point C is the position where the bore front, CB, at time t, intersects the unbroken wave front, CH. After a short time Δt, the point C has advanced to J, where JK represents the wave crest. L is the foot of the perpendicular from C to the new position of the bore (which lies along JP), M is the intersection of the extended bore front with the original line, CH, of wave crest, and N is the foot of the perpendicular from J to CH. The angle, NMJ, between the bore front and the unbroken wave crest is denoted as β. The distances $CL = c_b \Delta t$ and $JN = c_w \Delta t$, where c_b and c_w are the speeds of advance of the bore and the unbroken wave, respectively. In the right-angled triangle CLM, $CM = CL/\sin \alpha = c_b \Delta t/\sin \beta$, and in triangle JNM, $NM = JN/\tan \beta = c_w \Delta t/\tan \beta$. It follows therefore that $CN = CM - NM = c_b \Delta t/\sin \beta - c_w \Delta t/\tan \beta$, and the speed of the point C along the wave crest is $[CN/\Delta t = (c_b - c_w \cos \beta)/\sin \beta$. The same argument applies at break point B.

APPENDIX C

The near-breaking wave and the toe of the bore; $c_b = c_w$

In Figure 8 the wave crest and the toe of the bore are shown as CH and CQ, respectively, at time t, and as JK and JP, respectively, at $t + \Delta t$, a short time later; the point C is the break point at time t and J is the break point at time $t + \Delta t$. The line CH, representing the near-breaking wave crest advancing at speed, c_w, at time t, is straight and parallel to the toe of the bore moving at speed, $c_b = c_w$, in the region near Q. The curved shape of the toe between Q and C (or at the later time between P and J) can be seen in Figure 2A and 2B, and results from the movement of the toe of the foam down the front of the breaking wave in advance of the wave crest. The line $CR = NJ = c_w \Delta t$ indicates the distance of advance of the wave crest in time Δt, and the line $CL = RL + CR = (c_t + c_w)\Delta t$, indicates the advance of the toe of the foam produced by the breaking wave at point C, where c_t is the speed of the toe of the foam produced by the breaking wave relative to the moving wave; RL is the distance the toe of the foam has advanced relative to the wave crest. (The line JL is the location of the toe of the foam at time $t + \Delta t$ that is produced by the wave breaking at the break point as that point advances from C to J.) As in Section 3b, the speed of the break point along the

wave crest is given by CN/Δt and so $r = $ CN/NJ, or $\theta = $ angle CJN = angle LCN. The foam front, JL, will advance in a direction normal to the front, so that angle CJL = $\pi/2$. Then in triangle CNJ, CJ = NJ/$\cos\theta$, and in triangle LJC, CJ = CL$\cos\theta$. Equating these two expressions for CJ gives $\cos^2\theta = c_w/(c_w + c_t)$.

REFERENCES

Cheel, R.A. and A.E. Hay. 2008. Cross-ripple patters and wave directional spectra. J. Geophys. Res., *113*, C10009, doi:10.1029/2008JC004734, 2008.

Henderson, S.M., R.T. Guza, S. Elgar and T.H.C. Herbers. 2006. Refraction of surface gravity waves by shear waves. J. Phys. Oceanogr., *36*, 629–635.

Herbers, T.H.C., S. Elgar and R.T. Guza. 1999. Directional spreading of waves in the nearshore. J. Geophys. Res., *104* (C4), 7683–7693.

Herbers, T.H.C., M. Orzech, S. Elgar and R.T. Guza. 2003. Shoaling transformation of wave-frequency-directional spectra. J. Geophys. Res., *108*, C1, 3013, doi:10.1029/2001/JC001304, 2003.

Hisaki, Y. 2005. Ocean wave directional spectra estimation from an HF ocean radar with single antenna array: observation. J. Gephys. Res., *110*, C11004, doi:10.1029/2005/JC002881, 2005.

Kuik, A.J., G. Ph. van Vledder and L.H. Holthuusen. 1988. A method for routine analysis of pitch-and-roll buoy data. J. Phys. Oceanogr. *18*, 1020–1034.

Lighthill, M.J. 1978. Waves in fluids. Cambridge University Press, Cambridge, 504 pp.

Longuet-Higgins, M.S. and M.J.H. Fox. 1996. Asymptotic theory for the almost-highest solitary wave. J. Fluid Mech., *317*, 1–19.

Peregrine, D.H. 1983. Breaking waves on beaches. Annu. Rev. Fluid Mech., *15*, 149–178.

Pettersson, H.P., H.C. Graber, D. Hauser, C. Quentin, K.K. Kahma, W.M. Drennan and M.A. Donelan. 2003. Directional wave measurements from three wave sensors during the FETCH experiment. J. Geophys. Res., *108* (C3), 8061, doi:10.1029/2001JC001164, 2003.

Phillips, O.M. 1966. The dynamics of the upper ocean. Cambridge University Press, Cambridge, 261 pp.

Rapp, R.J. and W.K. Melville. 1990. Laboratory measurements of deep-water breaking waves. Phil. Trans. Roy. Soc. Lond. A, *331*, 735–800.

Tanaka, M. 1986. The stability of solitary waves. Phys. Fluids, *29*(3), 650–655.

Tanaka, M., J.W. Dold, M. Lewy and D.H. Peregrine. 1987. Instability and breaking of a solitary wave. J. Fluid Mech., *185*, 235–248.

Thorpe, S.A. 2005. The turbulent ocean. Cambridge University Press, Cambridge. 439 pp.

Thorpe, S.A. and A.J. Hall. 1993. Nearshore side-scan sonar studies. J. Atmos. Oceanic Tech. *10*, 778–783.

Thorpe, S.A., W.A.M. Nimmo Smith, A.M. Thurnherr and N.J. Walters. 1999a. Patterns in foam. Weather, *54*, 327–334.

Thorpe, S.A., W.A.M. Nimmo Smith, A. Graham and A.M. Thurnherr. 1999b. Patterns in foam and shallow tidal flows. In 'The wind-driven air-sea interface.' Proc. of Conference on Air-Sea Interaction, Sydney, January, 1999. Ed M.Banner. Publ:- School of Maths, UNSW, ISBN 0 7334 0586 X, pp 257–264.

Turner, J.S. and I.L. Turner. 2011. Foam patches behind spilling breakers. J. Mar. Res., *69*, 843–859. (Referred to as T&T in text.)